

Template-based synthesis of nickel oxide

N Mironova-Ulmane¹, A Kuzmin¹, I Sildos²

¹ Institute of Solid State Physics, University of Latvia, LV-1063 Riga, Latvia

² Institute of Physics, University of Tartu, 51014 Tartu, Estonia

E-mail: nina@cfi.lu.lv

Abstract. Nanocrystalline NiO has been produced using a facile template-based synthesis from nickel nitrate solutions using cellulose as a template. Thus obtained oxides were studied by scanning electron microscopy, x-ray diffraction, Raman scattering spectroscopy, photoluminescence spectroscopy and confocal spectromicroscopy. The filamentary/coral morphology of the samples has been evidenced and is built up of agglomerated nanocrystallites with a size in the range of about 26-36 nm. The presence of two-magnon contribution in Raman scattering spectra suggests the existence of antiferromagnetic ordering at room temperature. Finally, the observed near-infrared photoluminescence band at 850 nm has been tentatively attributed to the defect-perturbed Ni²⁺ states at the surface.

1. Introduction

Synthesis of materials using various template techniques becomes popular during last years due to simplicity and often low costs [1, 2, 3]. Such approach involves fabrication of the desired material within the pores or channels of a template that can be retained or removed thereafter. Several template materials have been utilized up to now to produce nanosized and mesoporous nickel oxide: eggshell membranes [4] or pinewood [5] as biotemplates, inorganic macroporous skeletons built up of close-packed polystyrene (PS) spheres [6], soft template octylamine [7], filamentous carbon [8], polyacrylonitrile [9], anodic aluminium oxide [10], cellulose [11] and agarose gel [12].

In this study we report on a facile template-based synthesis of nickel oxide from nickel nitrate solutions using cellulose as a template. We have found that thus obtained NiO samples retain the morphology of the template, which can be, however, influenced by the solution concentration. In particular, we will focus on the lattice dynamics, antiferromagnetic ordering and near-infrared photoluminescence of cellulose-templated NiO in comparison with micro- and nanocrystalline NiO produced by other methods [13, 14, 15].

2. Experimental

Cellulose-templated nickel oxide powder samples were produced by thermal decomposition of nickel nitrate hexahydrate salt at high temperature. First, aqueous solutions of nickel nitrate hexahydrate Ni(NO₃)₂·6H₂O were prepared at two concentrations (0.01 M and 0.05 M) to check the influence of the solution concentration on the amount (thickness) of nickel oxide layer surrounding the template framework. Next, the Whatman cellulose filter paper (Grade No. 2, Whatman 1002-110), used as a template, was impregnated with the solution, air dried at room temperature and heated for 1 hour at 650°C in tubular furnace to decompose nitrate and



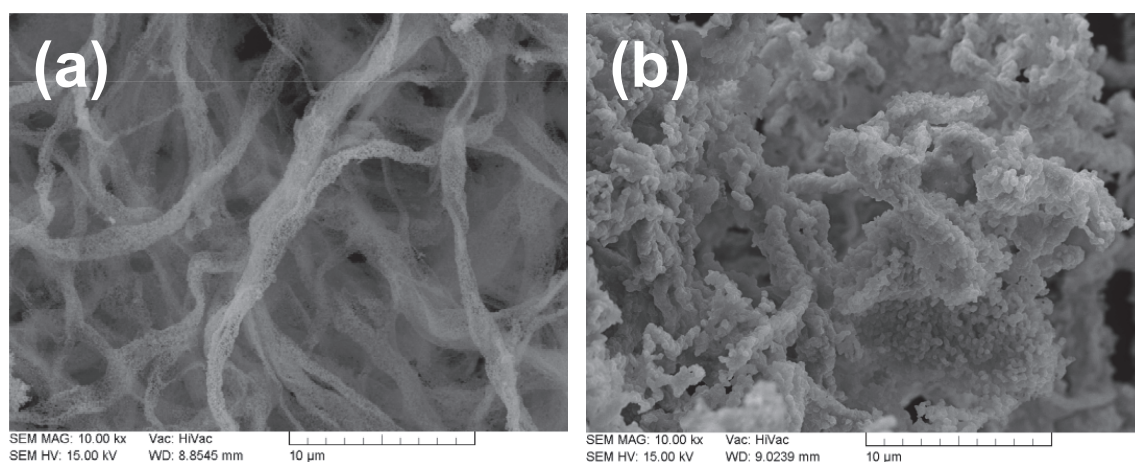


Figure 1. SEM images of cellulose-templated NiO: (a) 0.01 M and (b) 0.05 M.

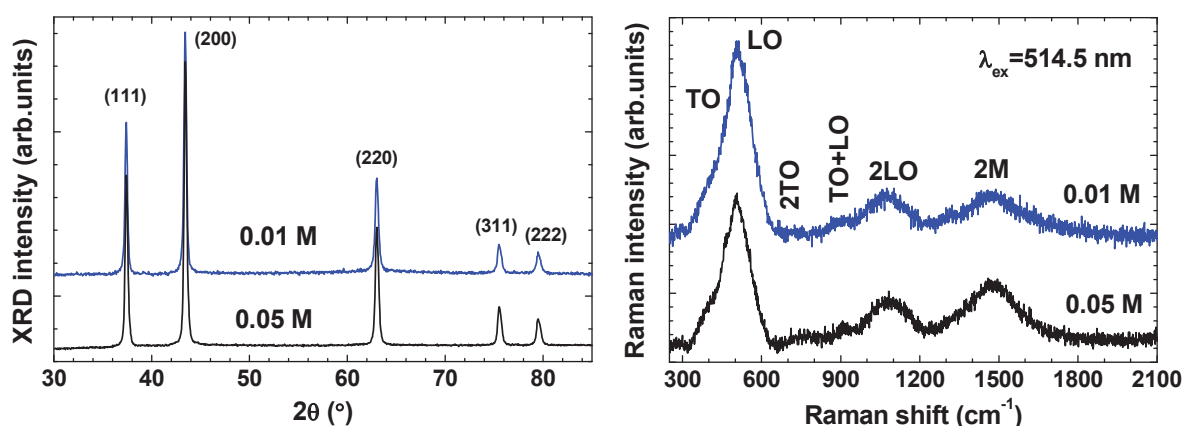


Figure 2. Room temperature x-ray diffraction patterns (left panel) and Raman scattering spectra (right panel) of cellulose-templated NiO.

to burn completely cellulose template. The final product, cellulose-templated NiO, was collected and used in further analysis. It has black color, which indicates the presence of nickel vacancies [16, 17].

The morphology of two samples was studied by scanning electron microscopy (SEM) using TESCAN MIRA microscope with secondary electron detector, whereas their phase composition was detected by x-ray diffraction using Bruker D2 PHASER θ - θ diffractometer equipped with copper anode x-ray tube.

Raman scattering spectra were measured in back-scattering geometry at room temperature (20°C) through 50× microscope objective using a Renishaw inVia micro-Raman spectrometer equipped with an argon laser (514.5 nm, max cw power $P_{\text{ex}}=10$ mW). The spectral signal was dispersed by 2400 grooves/mm diffraction grating onto a Peltier-cooled CCD detector.

Confocal microscopy and optical photoluminescence spectroscopy were performed using a confocal microscope with spectrometer Nanofinder-S (SOLAR TII). Spectra were collected in back-scattering geometry at room temperature (20°C). Diode-pumped solid-state (DPSS) Nd:YAG laser (532 nm, max cw power $P_{\text{ex}}=150$ mW) was used as the excitation source, and

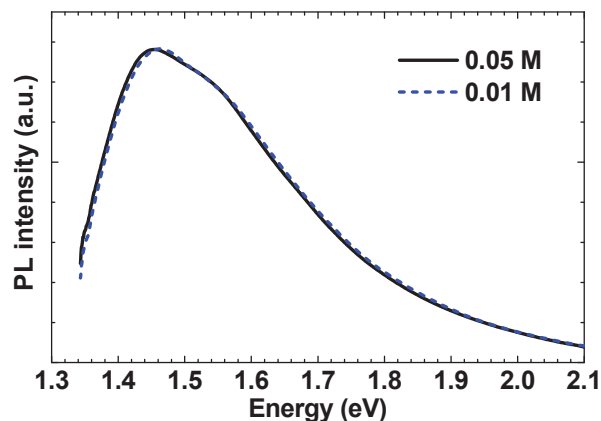


Figure 3. Photoluminescence spectra of cellulose-templated NiO at room temperature. The excitation laser wavelength was $\lambda_{\text{ex}} = 532$ nm.

the spectra were dispersed by 150 grooves/mm diffraction grating mounted in the 520 mm focal length monochromator. The elastic laser light component was eliminated by the edge filter (Semrock LP03-532RE). Peltier-cooled back-thinned CCD camera (ProScan HS-101H) was used as a detector in photoluminescence experiments, whereas the Hamamatsu R928 photomultiplier tube (PMT) was employed in confocal-spectral imaging experiments. To avoid possible sample damage, the laser power at the sample was controlled by a variable neutral-density filter with an optical density (OD) in the range OD=0-3.

3. Results and discussion

SEM images of cellulose-templated NiO are shown in figure 1. The grains with a size below 100 nm are observed in the sample produced from 0.01 M nitrate solution. They form filamentary structure surrounding cellulose framework, which was fired during annealing at 650°C. An increase of the nitrate solution concentration up to 0.05 M results in an agglomeration of grains into larger particles with a size of up to 500 nm, and the morphology becomes coral-like.

X-ray diffraction patterns of cellulose-templated NiO are shown in figure 2 (left panel). Five Bragg peaks (111), (200), (220), (311) and (222), due to the fcc NiO phase (JCPDS, No. 04-0835), are well visible. Their positions correspond to the average lattice parameter $a_0 = 4.174 \pm 0.003$ Å, which is in good agreement with the reported data for bulk NiO [18, 19]. The average size of nanocrystallites was calculated from the line broadening of the XRD patterns using the Scherrer's formula, and is equal to about 26–36 nm. This result suggests that the grains, observed by SEM in figure 1 for both samples, are composed of many crystallites.

The Raman scattering spectra of cellulose-templated NiO are shown in figure 2 (right panel). The temperature-dependent [20, 21, 22, 23] and pressure-dependent [24] Raman scattering studies of bulk NiO allow one to identify contributions from one-phonon (TO and LO modes), two-phonon (2TO, TO+LO, and 2LO modes) and two-magnon (2M) excitations. While in face-centered cubic (fcc) structure the first-order Raman scattering is forbidden, the intensity of one-phonon scattering (the band at ~ 500 cm^{-1}) is expected to increase significantly in defect-rich NiO [20]. In single-crystal, microcrystalline and nanocrystalline (down to 23 nm) NiO the intensity of the one-phonon band is usually smaller [14, 22, 25] or comparable [15, 20] to that of the two-phonon band at ~ 1100 cm^{-1} . However, a significant gain of the one-phonon band intensity was observed by us for smaller NiO nanoparticles with a size of 13 nm [15]. Thus, an increase of surface/bulk ratio and of defect concentration is responsible for the large intensity of

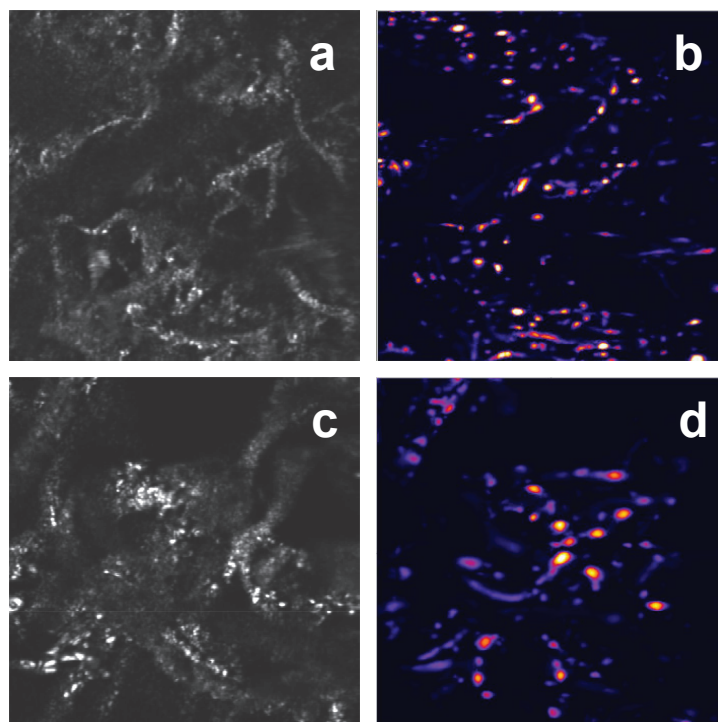


Figure 4. Confocal (a,c) and spectral (b,d) images of cellulose-templated NiO (0.01 M (a,b) and 0.05 M (c,d)). The image sizes are $98\ \mu\text{m}\times 95\ \mu\text{m}$. The spectral images were acquired at 850 nm.

the one-phonon band at $\sim 500\ \text{cm}^{-1}$. Finally, the presence of the two-magnon contribution (the band at $\sim 1500\ \text{cm}^{-1}$), having intensity comparable to the two-phonon 2LO band at $\sim 1100\ \text{cm}^{-1}$, indicates an existence of antiferromagnetic order at room temperature.

Luminescence of bulk NiO has been rarely studied in the past [13, 26, 27]. Two broad photoluminescence (PL) bands have been detected in [13] at 1.46 eV (850 nm) and 2.4 eV ($\sim 513\ \text{nm}$) in green colored NiO and $\text{Ni}_c\text{Mg}_{1-c}\text{O}$ ($c=0.95, 0.98, 0.99$) solid solutions under the low-energy laser excitation. At the same time, two broad emission bands, violet at 3.2 eV and green at 2.6 eV, have been observed under vacuum ultraviolet (VUV) and soft x-ray (XUV) excitations in [27].

Room temperature PL spectra of cellulose-templated NiO, excited by 532 nm laser, are shown in figure 3. The broad near-infrared band peaks at $\sim 1.46\ \text{eV}$ (850 nm) and is identical in both samples. The band is similar to that observed by us previously in green colored NiO and $\text{Ni}_c\text{Mg}_{1-c}\text{O}$ solid solutions [13]. Since the black color of cellulose-templated NiO is due to the large concentration of nickel vacancies both in the bulk and at the surface [28], we tentatively attribute the origin of the PL band to the defect-perturbed Ni^{2+} states at the surface.

The intensity of near-infrared PL band at $\sim 1.46\ \text{eV}$ (850 nm) was further used for mapping of a distribution of photoluminescence centers in cellulose-templated NiO samples. The confocal and spectral images were simultaneously acquired at 532 nm and 850 nm wavelengths, respectively, and are shown in figure 4. The image scanning was performed in the XY directions using two high-speed galvanometer-based mirror scanners, and the optical signals were detected by two PMTs. The confocal images give information on the reflectivity of the sample surface at 532 nm and evidence clearly the filamentary/coral structure of two samples. The spectral images show non-homogeneous spacial distribution of photoluminescence centers: the PL intensity is

larger at bright points. Note that the location of bright regions in confocal images differs from that with stronger PL intensity in spectral images, supporting their different origin. The heterogeneous distribution of the PL signal can be explained by particular excitation conditions at the sample points leading to PL nonradiative quenching, for example, due to local temperature variation upon laser heating.

4. Conclusions

Nanocrystalline NiO was synthesized from 0.01 M and 0.05 M nickel nitrate solutions by template-based method using cellulose as a template. Thus obtained NiO powders possess filamentary morphology of the template, have crystallites size in the range of about 26-36 nm and are antiferromagnetically ordered at room temperature. The large amount of nickel vacancies is responsible for the black color of the samples. Finally, the near-infrared photoluminescence band was observed at 1.46 eV (850 nm) in both samples at room temperature under 532 nm laser excitation and is tentatively attributed to the defect-perturbed Ni²⁺ states located at the surface. The distribution of the photoluminescence centers is non-homogeneous as is evidenced by confocal spectromicroscopy.

Acknowledgments

This work was supported by Latvian Science Council Grant no. 187/2012.

References

- [1] Huczko A 2000 *Appl. Phys. A* **70** 365
- [2] Wade T L and Wegrowe J E 2005 *Eur. Phys. J. Appl. Phys.* **29** 3
- [3] Jones M R, Osberg K D, Macfarlane R J, Langille M R and Mirkin C A 2011 *Chem. Rev.* **111** 3736
- [4] Rath M K, Choi B H, Ji M J and Lee K T 2014 *Ceram. Int.* **40** 3295
- [5] Liu Z, Fan T and Zhang D 2006 *J. Am. Ceram. Soc.* **89** 662
- [6] Yan H, Blanford C F, Holland B T, Parent M, Smyrl W H and Stein A 1999 *Adv. Mater.* **11** 1003
- [7] Shi J and Wu E 2013 *Micropor. Mesopor. Mater.* **168** 188
- [8] Ermakova M A, Ermakov D Y, Lebedev M Y, Rudina N A and Kuvshinov G G 2000 *Catal. Lett.* **70** 83
- [9] Qiu Y, Yu J, Zhou X, Tan C and Yin J 2008 *Nanoscale Res. Lett.* **9** 173
- [10] Needham S A, Wang G X and Liu H K 2006 *J. Power Sources* **159** 254
- [11] Duma V, Popp K, Kung M, Zhou H, Nguyen S, Ohyama S, Kung H and Marshall C 2004 *Chem. Eng. J.* **99** 227
- [12] Kim G P, Park S, Nam I, Park J and Yi J 2013 *J. Power Sources* **237** 172
- [13] Kuzmin A, Mironova-Ulmane N and Ronchin S 2003 *Proc. SPIE* **5122** 61
- [14] Cazzanelli E, Kuzmin A, Mariotto G and Mironova-Ulmane N 2003 *J. Phys.: Condens. Matter* **15** 2045
- [15] Mironova-Ulmane N, Kuzmin A, Grabis J, Sildos I, Voronin V I, Berger I F and Kazantsev V A 2011 *Solid State Phenom.* **168-169** 341
- [16] Sato H, Minami T, Takata S and Yamada T 1993 *Thin Solid Films* **236** 27
- [17] Kohmoto O, Nakagawa H, Isagawa Y and Chayahara A 2001 *J. Magn. Magn. Mater.* **226230** 1629
- [18] Slack G A 1960 *J. Appl. Phys.* **31** 1571
- [19] Kuzmin A and Mironova N 1998 *J. Phys.: Condens. Matter* **10** 7937
- [20] Dietz R E, Parisot G I and Meixner A E 1971 *Phys. Rev. B* **4** 2302
- [21] Lockwood D, Cottam M and Baskey J 1992 *J. Magn. Magn. Mater.* **104-107** 1053
- [22] Pressl M, Mayer M, Knoll P, Lo S, Hohenester U and Holzinger-Schweiger E 1996 *J. Raman Spectrosc.* **27** 343
- [23] Grimsditch M, McNeil L E and Lockwood D J 1998 *Phys. Rev. B* **58** 14462
- [24] Massey M J, Chen N H, Allen J W and Merlin R 1990 *Phys. Rev. B* **42** 8776
- [25] Mironova-Ulmane N, Kuzmin A, Steins I, Grabis J, Sildos I and Pärns M 2007 *J. Phys.: Conf. Ser.* **93** 012039
- [26] Mochizuki S and Saito T 2009 *Physica B* **404** 4850
- [27] Sokolov V I, Pustovarov V A, Churmanov V N, Ivanov V Y, Gruzdev N B, Sokolov P S, Baranov A N and Moskvina A S 2012 *Phys. Rev. B* **86** 115128
- [28] Ferrari A M, Pisani C, Cingolani G, Giordano L and Pacchioni G 2007 *J. Chem. Phys.* **127** 174711